

Supplementary Information for:

**Lipid Regulated Intramolecular Conformational Dynamics of
SNARE-Protein Ykt6**

*Yawei Dai^{1, 2}, Markus Seeger³, Jingwei Weng⁴, Song Song^{1, 2}, Wenning Wang⁴, Yan-Wen Tan^{1, 2, *}*

¹Department of Physics, Fudan University, 200433, Shanghai, P.R. China;

²State Key Laboratory of Surface Physics, Fudan University, 200433, Shanghai, P.R. China

³Institute of Biophysics, Goethe-University Frankfurt Max-von-Laue-Str. 1, 60438, Frankfurt/Main, Germany

⁴Shanghai Key Laboratory of Molecular Catalysis and Innovative Materials, Department of Chemistry and Institutes of Biomedical Sciences, Fudan University, 220 Handan Rd., 200433, Shanghai, P.R. China;

**Correspondence should be addressed to: ywtan@fudan.edu.cn.*

Note 1: Design of rYkt6 Δ C FRET construct

Single molecule FRET (smFRET) is a direct and powerful technique for demonstrating the conformational changes between the longin domain and the SNARE core of rYkt6 Δ C. Nevertheless, for smFRET measurements to perform well, the distances to be determined have to fall around the *Förster* radii R_0 of a chosen FRET pair since smFRET measurements are most sensitive there. The two labeling sites on the molecule, rYkt6 Δ C, has to be chosen such that the distances between them will optimally report any conformational changes between the longin domain and the SNARE core.

There is a native Cysteine residue, C66, in the sequence of Ykt6 from *Rattus norvegicus* besides the CCAIM terminal. To minimize the perturbation of the original construct, we reserved this C66 in the longin domain as one of the FRET labeling sites. We then narrowed down our labeling site selection to the central part of the core domain. To choose the proper site, we fetched the longin domain sequences from Pfam and UniProt, ran multiple sequence alignment with ClustalWS, and calculated the conservation scores for each residue on rYkt6. Residues with low conservation scores was chosen as potential labeling sites. We have chosen E175 as our labeling residue on rYkt6 Δ C. Since the only crystal structure of rYkt6 available (PDB-ID: 3KYQ) is in the closed form bound with DPC, we used MD simulation result to predict an open structure. Full length of rYkt6 Δ C has 193 amino acids (Figure S1a), and the yielded distances between predicted label sites (C66 and E175C) are in the range of 20 Å and 62 Å for the closed and open conformations respectively. In this work we have chosen two different FRET pairs, Alexa 555/647 and Alexa 488/647, for smFRET and FCCS experiments, respectively. The *Förster* radii R_0 for these two pairs are 51 Å and 56 Å, which is suitable for reporting conformational changes between 20 Å and 62 Å. As a remark, previous work *Hasegawa et al. 2004* found that targeting function of Ykt6 is regulated by its longin domain (sequence: 1-137) and normal Ykt6 requires a soluble intermediate. In our earlier attempts, we found that the native cysteine C66 is a possible site related to the solubility of Ykt6. The final construct Ykt6/E175C keeps the soluble features as the wild-type one. Although the native C66 labeling site is not fully exposed to solution in the structure with PDB id 3KYQ, the construct rYkt6 E175C can be readily doubly labeled which is observed in single-molecule experiment. (see Figure S2).

Note 2: Structure diversity analyzed by MD simulations at a longer distances range

As the Cys66-Glu175 C α distance falls within longer distance range, i.e. 3.2-3.9 nm, more prominent structural variability of the SNARE core was observed while the longin domain retains its structure. The conformations were divided into 49 clusters with a cutoff of 1.1 nm (Figure S7). The SNARE core becomes more stretched and less compact. The positions of the Glu175 C α are obviously distributed in a larger space than that of the 'closed' state, ranging around the α A helix, the β C- β D turn, the α D helix and the β D- β E turn (Figure S8(a), (b)). In spite of the more extended conformations in the 'open' state, two clusters were still found with the longin-SNARE BSA of more than 12 nm². The 1st cluster adopts a similar α G orientation as the 3rd and 5-8th clusters of the 'closed' state with the helix lying parallel with α A (Figure S8(c)). The 2nd cluster shows an antiparallel orientation between the α G and α A helices, reminiscent of the 9th cluster of the 'closed' state (Figure S8(d)). The N-terminus of α G helix is uncoiled in these two clusters, resulting in the longer distance between Glu175 and Cys66. We also inspect the centre structures with the smallest BSA (Figure S8(e-j)). In these structures, the α G helix is more than 0.9 nm away from the α A helix and has little contact with the longin domain. Nevertheless, the α G helix tends to pack with SNARE core itself in the last six clusters, placing its C-terminus in the vicinity of the α E helix. The backbone hydrogen bond interactions between β C and β F strands could be disrupted in the open state as in the last two clusters (Figure S8(i-j)). The disruption further reduces the BSA, providing extra conformational flexibility to the SNARE core. Though the open state is more disordered, the α G- α A packing is still observed, indicating the stability of the secondary structures.

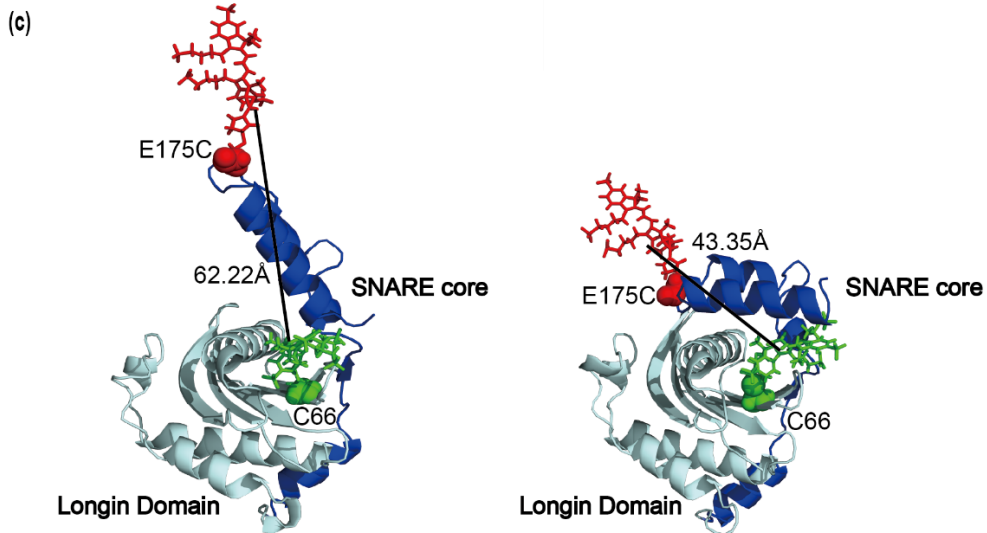
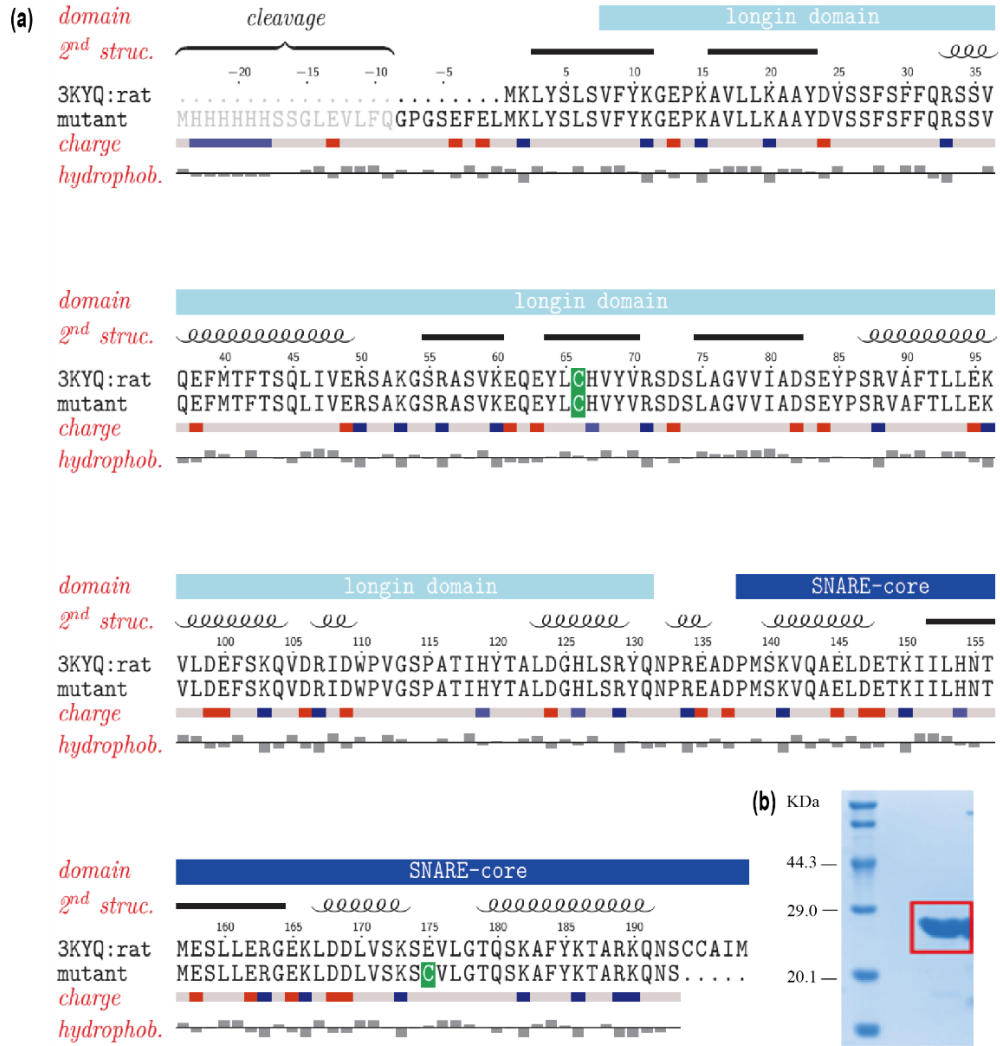


Figure S1. Sequence, purification, and labeling strategy of our FRET construct rYkt6 Δ C. (a) Amino acid sequence of rYkt6 Δ C and the modified FRET-construct; The chosen labeling sites are C66 and E175C (highlighted in green and red). (b) SDS-PAGE gel showing the purified rYkt6 Δ C protein used in our studies. The red box points out the molecular weight of rYkt6 Δ C at 24.6 KDa. (c) Two structures predicts by our Molecular Dynamics (MD) simulations showing the structures of doubly labeled Ykt6 in open (left) and closed (right) states. Both structures are simulated based on PDB structure 3KYQ, which is closer to the closed form. Structures of dyes are simulated with assumed structures of Alexa 555 (green) and Alexa 647 (red).

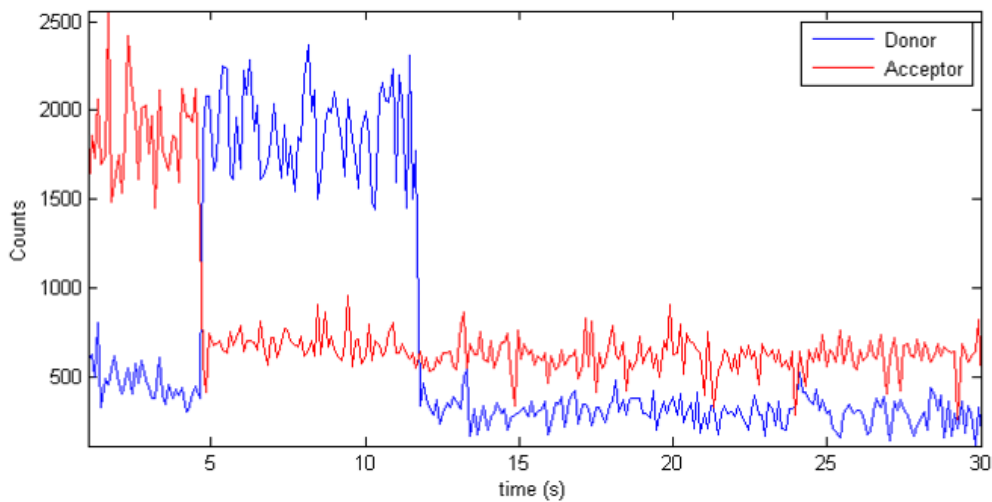


Figure S2. Single intensity vs. time trajectory of rYkt6 Δ C. The rYkt6 Δ C molecule is selected by the Co-localization method. The intensity vs. time trajectory of the chosen molecule is shown in Fig. S2. We impose a strict screening procedure to make sure each molecule taken into our data pool are labeled with one FRET pair (Alexa 555/647) as shown in Fig. S2. The blue curve stands for donor channel and the red curve stands for acceptor channel.

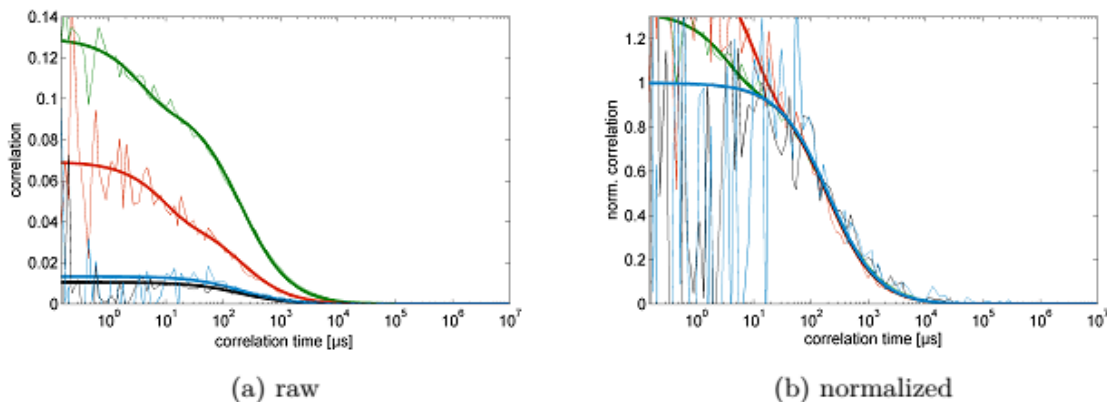


Figure S3. Correlations of double-labeled Poly-Proline (green: AC-d, red: AC-a, black: CC- da, blue: CC-ad). From Fig. S3(a) we found that all ACs (Autocorrelation) and CCs (Crosscorrelation) are obviously measurable. Regarding the correlation amplitude, the measurements confirms the expectations of a high amplitude of the AC-d (Autocorrelation Donor), a lower amplitude of acceptor and even lower amplitudes for the CCs. Furthermore the similarity of the CC shows the symmetry of the CCs. Fig. S3(b) shows that the normalized correlations owning the same correlation decay. This confirms that there is no time dependent difference between the four correlations. Since Poly-Proline₁₅ can be seen as a rigid molecule without intramolecular conformational dynamics, these measurements are consistent with theoretical expectations. Regarding the yielded Poly-Proline fitting results shown in tab. S1 , one can use the p-value marking the ratio of lateral to axial dimensions of the focal region for further measurements. The threshold of this parameter were set to 6.85 as the lower and 6.9 as the upper boundary conditions.

correlation	N	f	τ_D	p	τ_T
AC-d	10.187	0.243	198.393	6.847	3.480
AC-a	23.519	0.387	190.011	6.904	9.086
CC-da	94.974		197.182	6.864	
CC-aa	74.980		202.461	6.877	

Table S1: Fitting parameters of Poly-Proline

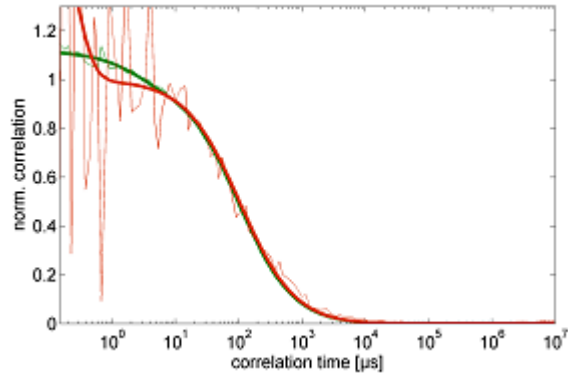


Figure S4. Normalized correlations of Rhodamine 6G with 1 nm and 5 nm (green: AC-d, red: AC-a). Rhodamine 6G was used as a simple reference sample to calculate the dimension of the focal region. In Fig. S4, both correlation functions coincide with each other beyond 10 μ s. From the fitting results one can calculate the dimensions of the focal region by using $\mu^2 = 4 \cdot D \cdot \tau_D$ with μ as the lateral dimension of the focus, D as the specific diffusion coefficient of the sample and τ_D as the average transit time through the focus. This leads to the focal dimensions of 4.07 μ m x 0.59 μ m.

correlation	N	f	τ_D	p	τ_T
AC-d	4.886	0.106	99.238	6.900	2.361
AC-a	27.236	0.661	104.901	6.900	0.157

Table S2. Fitting results of Rhodamine 6G

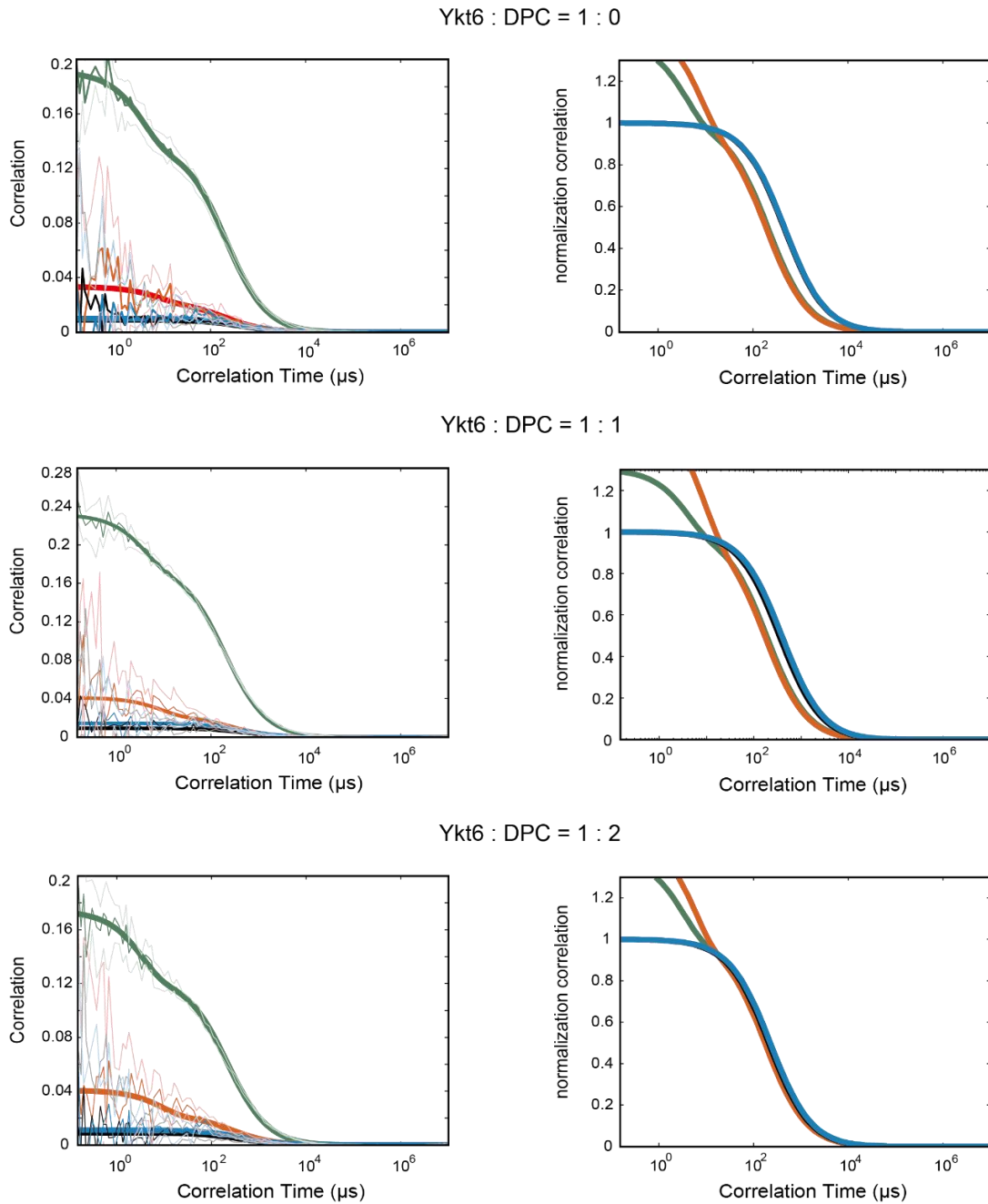


Figure S5. DPC concentration ratio gradient of double-labeled Ykt6 (green: AC-d, red: AC-a, black: CC- da, blue: CC-ad). Left side of Fig. S5 shows the raw data of correlations of double-labeled Ykt6. The normalized correlation data on the right side of Fig. S5 shows, that with increasing amount of DPC the time shift between both AC and the CC decreases and nearly vanishes at a concentration ratio of Ykt6 1:2 DPC. This DPC concentration ratio gradient presents that 1:2 ratio is the saturate concentration forces Ykt6 into a stable state.

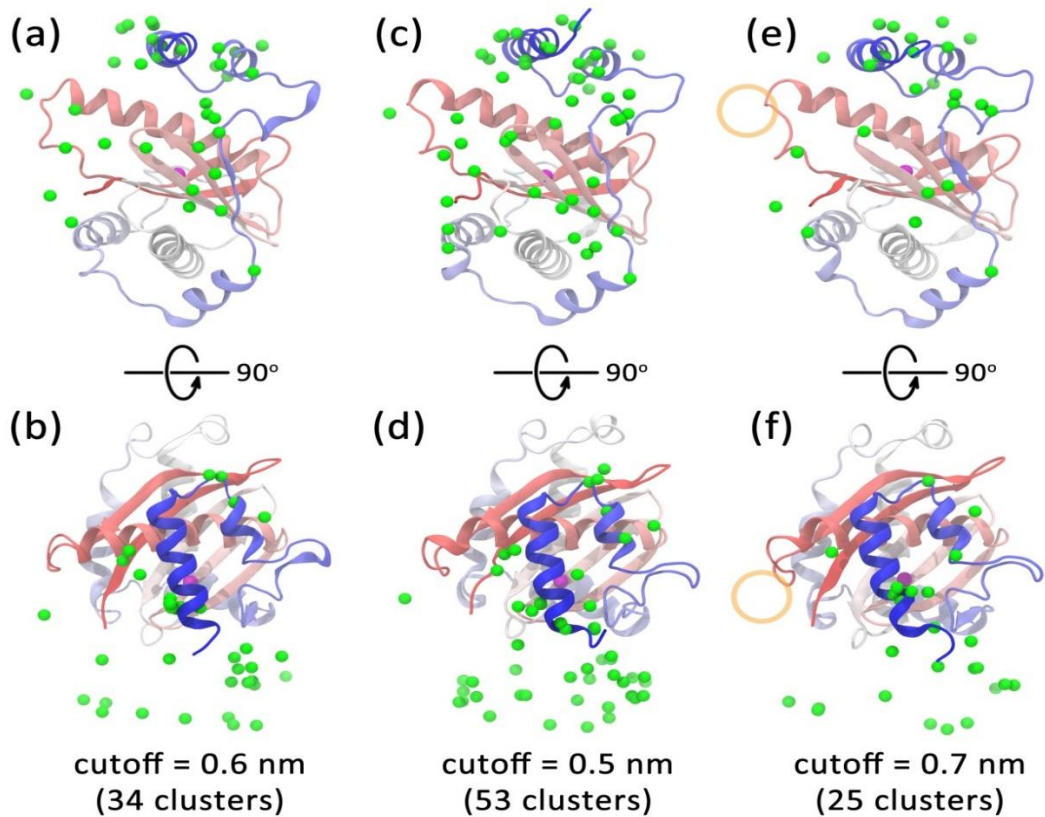


Figure S6. Cluster center structures of the snapshots with shorter Cys66-Glu175 distance in the metadynamics simulations using different cutoff values. The protein is represented by the cartoon mode and is coloured from red to blue. The C α atoms of Glu175 in the cluster center structures are represented as green balls and the C α atom of Cys66 is represented as magenta ball. Different cutoff values are used in the clustering analysis. Larger cutoff values lead to fewer clusters and when the cutoff equals 1.0 nm, a characteristic center structure is neglected as marked by the orange circle.

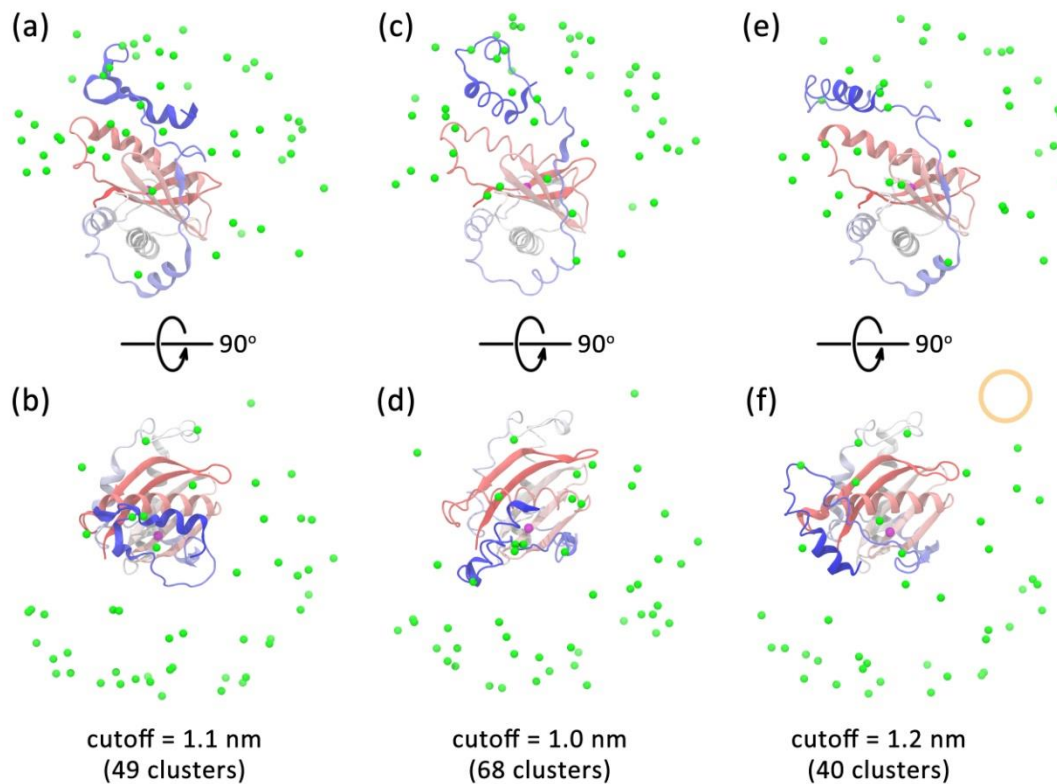


Figure S7. Cluster center structures of the snapshots with longer Cys66-Glu175 distance in the metadynamics simulations using different cutoff values. The protein is represented by the cartoon mode and is coloured from red to blue. The $C\alpha$ atoms of Glu175 in the cluster center structures are represented as green balls and the $C\alpha$ atom of Cys66 is represented as magenta ball. Different cutoff values are used in the clustering analysis. Larger cutoff values lead to fewer clusters and when the cutoff equals 1.0 nm, a characteristic center structure is neglected as marked by the orange circle.

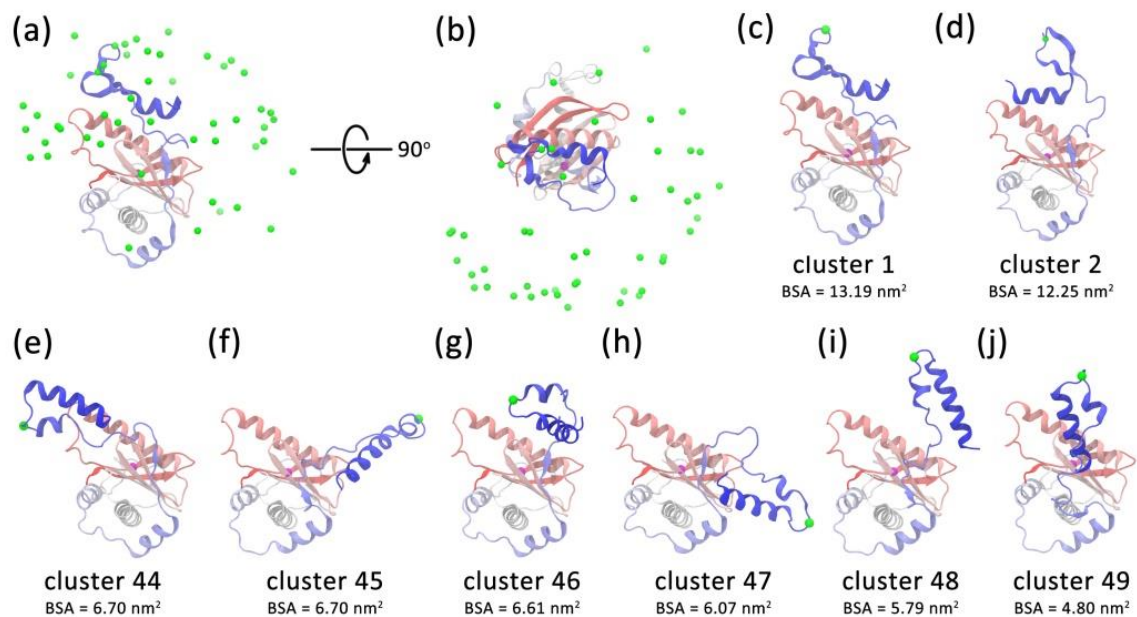


Figure S8. Representative structures with longer Cys66-Glu175 C α distance from the MD simulation. Front view (a) and top view (b) of the cluster centre structures of the snapshots with the Cys66-Glu175 distance ranging from 3.2 to 3.9 nm in the metadynamics simulations using a cutoff of 0.6 nm. The protein is represented by the cartoon mode and is coloured from red to blue. The C α atoms of Glu175 in the cluster centre structures are represented as green balls and the C α atom of Cys66 is represented as magenta ball. (c)-(d) The centre structures with the BSA between longin domain and SNARE core of more than 12 nm². (e)-(j) The six centre structures with the smallest BSA.